

# Theoretical Studies of the Effects of $\alpha$ -methylation and $\beta$ -methylation on the Gas - Phase Kinetics of Thermal Decomposition of Allyl formates

Adejoro, I. A.\* Onyia, K. K. Akintemi, E. O.  
Department of Chemistry, University of Ibadan, Ibadan, Nigeria

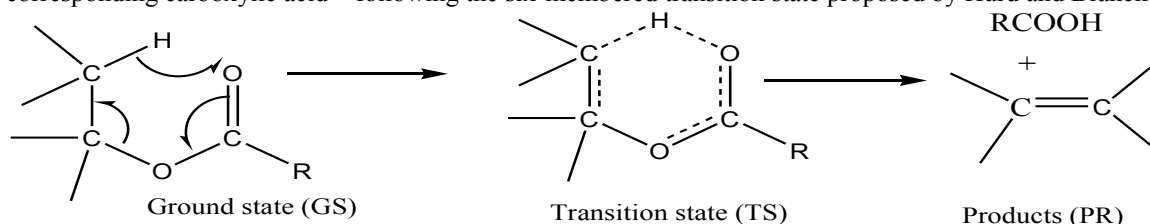
## Abstract

The gas phase pyrolytic reaction of allyl formate (I), its  $\alpha$ -methylated compound (II) and  $\beta$ -methylated compound (III) were studied theoretically with semi-empirical PM3, hatree-fock HF/3-21G and density functional theory, DFT (B3LYP/6-31G\*) methods. The decomposition of these compounds proceeds by a concerted [1, 5] hydrogen shift through a six-centered transition state (TS) geometry. The overall result of calculations shows that the reactivity of the thermal decomposition increases consequent to steric releasing effect in the transition state by the methyl group at the  $\alpha$ -position, hence it is rate enhancing while reactivity decreases upon  $\beta$ -methylation, decreasing the rate of reaction. Also, it is found that rate enhancement due to C-O bond stretching in the formation of TS is more significant as a rate determinant than the acidic nature of the eliminated formyl hydrogen.

**Keywords:** Kinetics, hydrogen shift, allyl formate, mechanism,  $\alpha$ -, $\beta$ -methylation

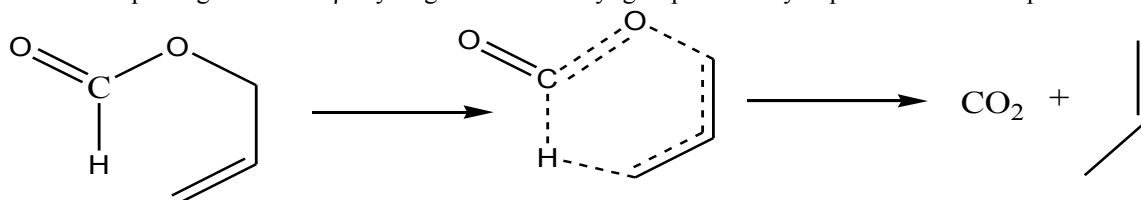
## 1.1 Introduction

The gas-phase thermal decomposition of esters has been extensively studied experimentally<sup>[1-4]</sup> and theoretically<sup>[5-7]</sup>, and the reaction is known to proceed in a concerted process through a six-centered transition state (TS) type of mechanism as described in reaction scheme 1. A number of studies have revealed that many simple esters containing non-vinylic  $\beta$ -hydrogen in the alkyl portion decompose to give one or more olefinic products with their corresponding carboxylic acid<sup>[8]</sup> following the six-membered transition state proposed by Hurd and Blunck<sup>[9]</sup>.



### Scheme 1: General mechanism for pyrolysis in simple esters

An interesting ester of formic acid where the alkyl group is replaced with vinylic group, is allyl formate which when pyrolyzed in static system produces propene and carbon (IV) oxide<sup>[10]</sup>. The elimination process is an intramolecular mechanism involving 1,5 transfer of the formyl hydrogen atom as shown in scheme 2. The aim of this study is to use semi-empirical, Hatree-Fock approximations and density functional computational approaches in SPARTAN to compute the kinetics, thermodynamics and the mechanism of the pyrolysis of allyl formate and the effect of replacing an  $\alpha$  and a  $\beta$ -hydrogen with a methyl group at the allylic portion of the compound.

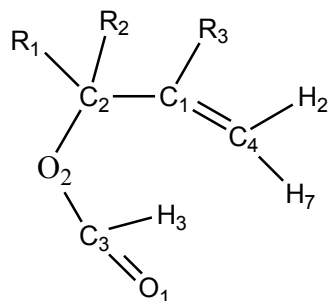


### Scheme 2: Mechanism of the intramolecular [1, 5] hydrogen shift in allyl formate.

## 1.2 Computational Procedure

The Semi-empirical PM3, Hatree-fork (HF/3-21G) and DFT (B3LYP/6-31G\*) computational methods were used in this work. Conformational search was carried out on the structures using Molecular Mechanics Force Field (MMFF) in aqueous medium which is quite successful in designating low energy conformers as well as providing quantitative estimates of conformational energy differences to obtain the structure with the lowest energy value which is an indication of the stability of the molecule<sup>[11]</sup>. The allyl formate and its  $\alpha$ -, $\beta$ -methylated compounds have nine conformers each with their global minima having energies -278.62 kJmol<sup>-1</sup>, -34.10 kJmol<sup>-1</sup> and -25.45

$\text{kJmol}^{-1}$  respectively. Geometry optimization was performed on the ground state (GS), the transition state (TS) and the products (PR) to obtain the geometric parameters such as bond length, bond angle, dihedral, atomic charges and some thermodynamics parameters like enthalpy, entropy and Gibb's free energy of the reaction. The geometry of the allyl formates is demonstrated in scheme 3, where  $\text{H}_3$  is the formyl hydrogen that will be transferred in a [1, 5] hydrogen shift mechanism.



**Scheme 3:** Geometry of the studied allyl formates.  $\text{R}_1$ ,  $\text{R}_2$  or  $\text{R}_3 = \text{H}$  or alkyl group

**Table 1:** Esters Studied in this Work

Designation	Non – hydrogen substituent	Nomenclature
I	-	Allyl formate
II	$\text{R}_1$ or $\text{R}_2 = \text{CH}_3$	$\alpha$ – methyl allyl formate
III	$\text{R}_3 = \text{CH}_3$	$\beta$ – methyl allyl formate

The transition state structures were identified through the guess-transition state as suggested by the mechanism of the transition state structure in SPARTAN'10 [20]. The proposed structures were optimized and subjected to the two tests necessary for ascertaining how a practical geometry corresponds to a saddle point (transition structure) and that this saddle point corresponds to the reactants and products. The tests include the Hessian matrix of second-energy derivations with respect to coordinates that yields only one imaginary frequency which will be in the range of  $400$  to  $2000 \text{ cm}^{-1}$  and the normal coordinates which corresponds to the imaginary frequency smoothly correcting the reactants and products.

### 1.2.1 Calculations

The enthalpy calculated by the modeling software is solely based on statistical mechanics and does not take into account the ground state energy which has significant contribution to the total energy of the molecule. However, a function of the software is to calculate the ground state energy (GSE) using quantum mechanics. Therefore, we can simply take the sum of the enthalpy and the ground state energy equal to the overall energy of the molecules or total enthalpy and calculate the heat of reaction by taking the difference between the product and reactant overall energies.

According to Spartan Guide to calculations [19], the enthalpy of a compound will be defined as:

$$H = GSE + H^{sm} \quad (1)$$

$H^{sm}$  is the statistically mechanically calculated enthalpy.

If the above equation is substituted into the initial definition of the heat of reaction, we have:

$$\Delta H_{rxn} = (GSE_{product} + H_{product}) - (GSE_{reactant} + H_{reactant}) \quad (2)$$

The enthalpy of reaction was calculated at  $710.5\text{K}$ .

The enthalpy of activation ( $\Delta H^\ddagger$ ) was obtained by subtracting the enthalpy of reactant from the enthalpy of transition state at  $710.5\text{K}$ .

$$\Delta H^\ddagger = (GSE_{transition} + H_{transition}) - (GSE_{reactant} + H_{reactant}) \quad (3)$$

According to the transition state theory for a unimolecular reaction, activation energy ( $E_a$ ) is given as:

$$E_a = \Delta H^\ddagger + RT \quad (4)$$

The entropy of activation ( $\Delta S^\ddagger$ ) was calculated at  $710.5\text{K}$  by taking the difference of transition state and reactant entropies that is:

$$\Delta S^\ddagger = S_{transition} - S_{reactant} \quad (5)$$

$\Delta S^\ddagger$  value was used to calculate Arrhenius pre-exponential factor using the relation;

$$A = (e^m k_b T / h) \exp \{(\Delta S^\ddagger / R)\} \quad (6)$$

$m$  is the molecularity of the reaction,  $k_b$  is the Boltzmann constant and  $h$  is the Planck constant.

The first order coefficient  $k(T)$  was calculated using transition state theory (TST) [12] assuming that the transition coefficient is unity as shown in the following equation:

$$k(T) = \frac{k_b T}{h} \exp \left[ \frac{-\Delta G^\ddagger}{RT} \right] \quad (7)$$

$\Delta G^\ddagger$  is the Gibbs free energy change between the reactant and the transition state, it was calculated using the following relation:

$$\Delta G^\ddagger = G_{\text{transition}} - G_{\text{reactant}} \quad (8)$$

Arrhenius rate equation is given as:

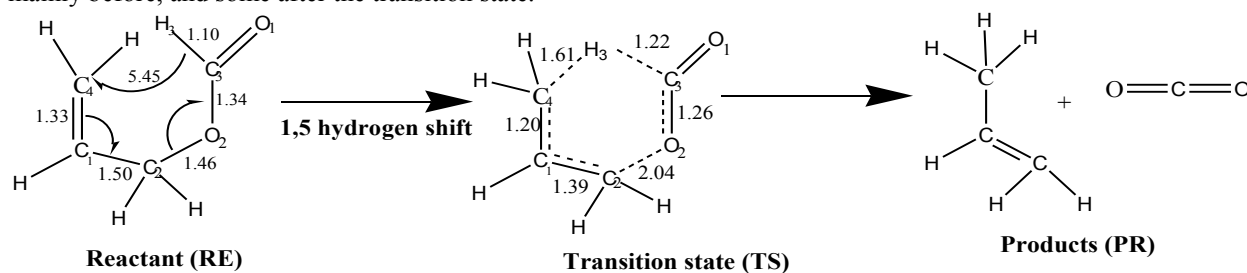
$$k(T) = \frac{k_B T}{h} \exp\left[\frac{-E_a}{RT}\right] \quad (9)$$

### 1.3 Results and Discussion

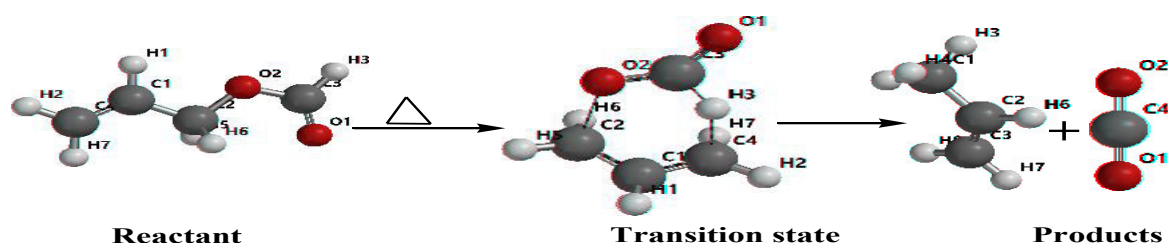
Using the semi-empirical, hartree-fock and Density Functional Theory methods, the geometry of the reactant(s), transition state(s) and product(s) was predicted and shown below in schemes IV and V. Experimental works reported by Hurd and Blunk<sup>[9]</sup>, Depuy and King<sup>[13]</sup>, Mcgreer and Chiu<sup>[14]</sup>, suggested that the thermal decomposition of esters passes through a six-membered ring transition state if hydrogen of the alkyl substituent at the  $\alpha$ -position is available for abstraction by acyl group.

The reaction pathway of allyl formate is depicted in scheme 4 where the relevant atom numbering is also indicated. This study suggests that the gas-phase decomposition of allyl formate to give propene and carbon (IV) oxide occurs by a concerted asynchronous mechanism, that is, processes that led to the intermediate are concerted but the rate determining process is not synchronous but delayed<sup>[15]</sup>.

As shown in scheme 4, two bonds that are breaking off, C<sub>2</sub>-O<sub>2</sub> and C<sub>3</sub>-H<sub>3</sub>, are seen to stretch from 1.455Å and 1.10Å in the RE to 2.04Å and 1.23Å respectively in the TS (Table 3). In the transition state, C<sub>4</sub>-H<sub>3</sub> bond is almost fully formed showing that this process is a two-stage reaction in which some changes in bonding took place mainly before, and some after the transition state.



Scheme 4: Reaction pathway



Scheme 5: Spartan ball and spoke model for the reaction pathway

#### 1.3.1 Geometry Parameters

Atomic charges are shown in Mulliken which according to Spartan calculation guide<sup>[19]</sup> is preferred because it gives simple and reasonable estimates of atomic charges. As the reaction progresses from reactant to product, the electron density at the carbonyl carbon C<sub>3</sub>, decreases, C<sub>3</sub> becoming more positive for the substrates. The negative charge on carbon C<sub>2</sub> increases in the transition state as the O<sub>2</sub>-C<sub>2</sub> bond breaks; this change is more noticeable for allyl formate (-0.102) and  $\beta$ -methyl allyl formate (-0.110) compared to  $\alpha$ -methyl allyl formate (-0.051). However, charge on oxygen O<sub>2</sub> undergoes very small change for the substrates, from reactant to transition state, carbon C<sub>2</sub> and C<sub>1</sub> bearing the methyl substituent increase in electron density in transition state, implying donation of electron density from the  $\alpha,\beta$ -methyl substituent. Tables 2 and 3 shows selected optimized geometric parameters (bond lengths, bond angles and dihedral angles) of reactants, transition states and products. They reveal that  $\alpha$ -methylation of allyl formate leads to greater O<sub>2</sub>-C<sub>2</sub> stretch in the TS. Principally,  $\alpha$ -methylation of allyl formate reflect on the charge density and bonds joined to the sites of substitution, that is charge density on C<sub>2</sub> and C<sub>2</sub>-O<sub>2</sub> and C<sub>1</sub>-C<sub>2</sub> bond lengths.

The methyl group has a positive (electron releasing) inductive effect, the methyl carbon being partially negative. The  $\alpha$ -methyl substitution facilitated electron movement from C<sub>2</sub>-O<sub>2</sub> bond into O<sub>2</sub>-C<sub>3</sub> bond. This increased the C<sub>1</sub>-C<sub>2</sub> bond length (1.496Å to 1.501Å), thereby lessening the developing double bond character.

**Table 2:** Atomic charges (q) and Bond length (d in Å) at selected atoms of reactant (RE), transition state (TS) and products (PR) for the decomposition of allyl formates at DFT/B3LYP/6-31G\* level.

Atom	Allyl formate				$\alpha$ – methyl allyl formate				$\beta$ – methyl allyl formate			
	RE	TS	PR	$\Delta q^*$	RE	TS	PR	$\Delta q^*$	RE	TS	PR	$\Delta q^*$
C <sub>1</sub>	-0.057	-0.053	-	0.004	-	-	-	-	0.211	0.197	0.219	-0.014
O <sub>2</sub>	-0.415	-0.420	-	-	-	-	-	-	-	-	-0.367	-0.005
C <sub>2</sub>	-0.095	-0.197	-	-	0.068	0.017	-	-	0.417	0.422	-0.400	-0.110
C <sub>3</sub>	0.391	0.495	0.730	0.104	0.392	0.460	0.733	0.068	0.115	0.225	0.727	0.077
H <sub>3</sub>	0.139	0.068	0.167	-	0.136	0.068	0.164	-	0.139	0.067	0.157	-0.072
C <sub>4</sub>	-0.331	-0.370	-	-	-	-	-	-	-	-	-0.503	-0.011
			0.490	0.039	0.337	0.368	0.491	0.031	0.389	0.400		
Bond	RE	TS	PR	$\Delta d^*$	RE	TS	PR	$\Delta d^*$	RE	TS	PR	$\Delta d^*$
C <sub>1</sub> -C <sub>2</sub>	1.496	1.389	1.335	-	1.501	1.395	1.337	-	1.504	1.392	1.338	-0.112
				0.107				0.106				
C <sub>1</sub> -C <sub>4</sub>	1.332	1.202	1.502	-	1.332	1.385	1.503	0.053	1.336	1.394	1.509	0.058
				0.130								
C <sub>2</sub> -O <sub>2</sub>	1.455	2.036	3.464	0.581	1.468	2.094	3.480	0.626	1.456	2.057	3.710	0.601
C <sub>3</sub> -O <sub>2</sub>	1.345	1.257	1.169	-	1.341	1.212	1.169	-	1.341	1.257	1.169	-0.084
				0.085				0.129				
C <sub>3</sub> -H <sub>3</sub>	1.101	1.226	3.690	0.125	1.101	1.212	3.565	0.111	1.101	1.226	4.122	0.216
C <sub>4</sub> -H <sub>3</sub>	5.450	1.610	1.098	-	5.271	1.665	1.098	-	5.416	1.602	1.094	-3.814
				3.840				3.606				

$$\Delta q^* = q^{(TS)} - q^{(RE)}; \Delta d^* = d^{(TS)} - d^{(RE)}$$

**Table 3:** Optimized Bond and Dihedral angles for both reactant (RE) and transition state (TS) for allyl formates at DFT/B3LYP/6-31G\* level.

Bond angle (°)	Allyl formate		$\alpha$ -methyl allyl formate		$\beta$ -methyl allyl formate	
	RE	TS	RE	TS	RE	TS
C <sub>1</sub> -C <sub>2</sub> -O <sub>2</sub>	107.90	102.57	106.14	100.02	108.34	101.50
C <sub>2</sub> -O <sub>2</sub> -C <sub>3</sub>	115.48	113.91	116.68	115.05	115.58	113.50
H <sub>3</sub> -C <sub>3</sub> -O <sub>2</sub>	108.93	109.81	108.72	109.23	108.95	109.27
H <sub>3</sub> -C <sub>3</sub> -C <sub>4</sub>	128.93	17.33	40.83	148.73	129.27	17.54
Dihedral angle (°)						
C <sub>2</sub> -O <sub>2</sub> -C <sub>3</sub> -O <sub>1</sub>	-0.36	173.19	0.69	173.27	0.19	-174.45
C <sub>2</sub> -O <sub>2</sub> -C <sub>3</sub> -H <sub>3</sub>	179.65	-7.61	-179.12	-7.30	-179.90	6.40

### 1.3.2 Activation Energy Correlation

Methyl substitution at the  $\alpha$ - carbon position of allyl formate lower the activation energy ( $E_a$ ) from 196.02kJmol<sup>-1</sup> to 177.07kJmol<sup>-1</sup>. This lowering of  $E_a$  is rate enhancing and the rate enhancement is generally ascribed to stabilization of C<sub>2</sub> bearing the methyl group by electron donating effect of the methyl group and steric acceleration of rate by the methyl group in TS. The explanation of the effect of  $\alpha$ -methylation on the rate is that  $\alpha$ -methyl substituent will tend to stabilize the six-centered transition state because of its polarity and substituents which are able to stabilize the growing charge centers of the activated complex. Thus, effecting reduction in the activation energies relative to the unsubstituted reactant. Also,  $\beta$ -methylation increases the activation energy ( $E_a$ ) from 196.02kJmol<sup>-1</sup> to 198.00kJmol<sup>-1</sup>, thereby reducing the rate of reaction. Because of the above reasons, it can therefore be concluded that rate enhancement due to C<sub>2</sub>-O<sub>2</sub> bond stretching in the formation of the transition state is more significant as a rate determinant than the acidic nature of the hydrogen that is eliminated.

The results of the kinetic parameter found experimentally for allyl formate are:

$E_{act} = 43.15 \pm 0.66$  kcalmol<sup>-1</sup> (180.5  $\pm$  2.9 kJmol<sup>-1</sup>); log A = 10.0  $\pm$  0.2 [17] and  $E_{act} = 43.0 \pm 0.9$  kcalmol<sup>-1</sup> (179.9  $\pm$  3.8 kJmol<sup>-1</sup>); log = 10.1  $\pm$  0.3 [18] while the calculated value for log A is 14.24, 14.21 and 14.15 respectively for PM3, HF/3-21G and DFT/B3LY/6-31G\* levels.

It is important to note that the reported experimental values of log A of the allyl formates are rather low for a six-centered cyclic transition state structure. Estimation of Benson *et al.* [12] about the values of A-factor from transition state theory should approximately be around 10<sup>9.0</sup> -10<sup>15.2</sup> for six-membered cyclic transition state geometry.

**Table 4:** Effect of  $\alpha$  – methylation on activation energy and reaction rate at 710.5K

Methods	Allyl formate $E_a(kJmol^{-1})$	$k(x10^{-1})$ ( $S^{-1}$ )	$\alpha$ -methyl allyl formate $E_a(kJmol^{-1})$	$k(x10^1)$ ( $S^{-1}$ )
PM3	194.57	8.81	174.98	2.23
HF/3-21G	194.70	7.91	174.37	1.63
DFT/B3LYP/6-31G*	196.02	5.53	177.07	0.99

**Table 5:** Effect of  $\beta$  – methylation on activation energy and reaction rate at 710.5K

Methods	Allyl formate $E_a(kJmol^{-1})$	$k(x10^{-1})$ ( $S^{-1}$ )	$\beta$ -methyl allyl formate $E_a(kJmol^{-1})$	$k(x10^{-1})$ ( $S^{-1}$ )
PM3	194.57	8.81	197.40	4.62
HF/3-21G	194.70	7.91	196.45	5.24
DFT/B3LYP/6-31G*	196.02	5.53	198.00	3.45

**Table 6:** Comparison of computed Arrhenius parameters and the experimental result for allyl formate

Methods	$E_a(kJmol^{-1})$	$\Delta H^\ddagger(kJmol^{-1})$	LogA
Experimental	180.75	174.84	10.00
PM3	194.57	188.66	14.24
HF/3-21G	194.70	188.79	14.21
DFT/B3LYP/6-31G*	196.02	190.11	14.15

**Table 7:** Thermodynamic and Arrhenius Parameters for the pyrolysis of Allyl formate

Methods	$\Delta H^\ddagger$ ( $kJmol^{-1}$ )	$\Delta G^\ddagger$ ( $kJmol^{-1}$ )	$\Delta S^\ddagger$ ( $Jmol^{-1}K^{-1}$ )	$E_a$ ( $kJmol^{-1}$ )	$k$ ( $x10^{-1}$ ) ( $S^{-1}$ )	A ( $x10^{14}$ ) ( $S^{-1}$ )	LogA
PM3	188.66	180.14	12.23	194.57	8.81	1.75	14.24
HF/3-21G	188.76	180.97	11.50	194.70	7.91	1.61	14.21
DFT/B3LYP/6-31G*	190.11	183.00	10.38	196.02	5.53	1.4	14.15

**Table 8:** Thermodynamic and Arrhenius Parameters for the pyrolysis of  $\alpha$  – methallyl formate

Methods	$\Delta H^\ddagger$ ( $kJmol^{-1}$ )	$\Delta G^\ddagger$ ( $kJmol^{-1}$ )	$\Delta S^\ddagger$ ( $Jmol^{-1}K^{-1}$ )	$E_a$ ( $kJmol^{-1}$ )	$k$ ( $x10^{-1}$ ) ( $S^{-1}$ )	A ( $x10^{14}$ ) ( $S^{-1}$ )	LogA
PM3	169.07	161.02	11.51	174.98	2.23	1.61	14.21
HF/3-21G	169.46	162.92	9.47	174.37	1.63	1.26	14.10
DFT/B3LYP/6-31G*	171.16	162.66	8.62	177.07	0.99	1.02	14.01

**Table 9:** Thermodynamic and Arrhenius Parameters for the pyrolysis of  $\beta$  – methallyl formate

Methods	$\Delta H^\ddagger$ ( $kJmol^{-1}$ )	$\Delta G^\ddagger$ ( $kJmol^{-1}$ )	$\Delta S^\ddagger$ ( $Jmol^{-1}K^{-1}$ )	$E_a$ ( $kJmol^{-1}$ )	$k$ ( $x10^{-1}$ ) ( $S^{-1}$ )	A ( $x10^{14}$ ) ( $S^{-1}$ )	LogA
PM3	191.49	183.68	10.82	197.40	4.62	1.48	14.17
HF/3-21G	190.54	182.72	10.57	196.45	5.24	1.43	14.16
DFT/B3LYP/6-31G*	192.09	185.70	9.21	198.00	3.45	1.22	14.09

#### 1.4 Conclusion

The gas-phase decomposition mechanisms of allyl formate,  $\alpha$ -methyl allyl formate and  $\beta$ -methyl allyl formate were investigated by means of density functional, hartree-fock and semi-empirical calculations. Available experimental data of the reaction were used to analyze the calculated parameters to propose a reasonable mechanism. The result shows that the reaction proceeds in a concerted non-synchronous six centered transition state mechanism. The theoretical results are in reasonable agreement with the experimental results. Also, reactivity of allyl formate increases with methyl substitution at  $\alpha$ -position and decreases upon  $\beta$ - methylation by electron donating effect of methyl group. This leads to steric acceleration of rate in TS for  $\alpha$ -methyl allyl formate and a decrease in the rate for  $\beta$ -methyl allyl formate.

#### References

1. A.T. Blades, The kinetics of the pyrolysis of ethyl and isopropyl formates and acetates, Can. J. Chem. 32 (1954) 366–372.
2. A.T. Blades, H.S. Sandhu, The Arrhenius factors for some six-center unimolecular reactions, Int. J. Chem. Kinet.

III (1971) 187–193.

3. R.F. Makens, W.G. Eversole, Kinetics of the thermal decomposition of ethyl formate, *J. Am. Chem. Soc.* 61 (1939) 3203–3206.
4. E. Gordon, S.J.W. Price, A.F. Trotman-Dickenson, The pyrolysis of tert.-butyl formate, *J. Chem. Soc.* (1957) 2813–2815.
5. (a) R. Taylor, *The Chemistry of the Functional Groups, Supplementary Volume B. Acid Derivatives*, ed., S. Patia, Wiley, London, (1979) p.880; (b) R. Taylor and M. P. Thorne, *J. Chem. Soc., Perkin Trans. 2* (1976) 799; (c) R. Taylor, *J. Chem. Soc., Perkin Trans. 2* (1972) 165; (d) S. de B. Norfolk and R. Taylor, *J. Chem. Soc., Perkin Trans. 2* (1976).
6. N. Al-Awadi, R. F. Al-Bashir, and O. M. E. El- Dosouqui, *J. Chem. Soc., Perkin Trans. 2* (1989) 576.
7. I.A. Adejoro, T.O. Bamkole, Semi-empirical quantum Mechanical, Molecular Orbital Method using MOPAC: Calculation of the Arrhenius parameters for the pyrolysis of some Alkyl Acetates *J. Appl. Sci.* 5(9) (2005) 1559 - 1563.
8. R. Taylor, In *chemistry of functional groups*, Patai S (ed). Wiley: Chinchester. (1986)
9. C.D. Hurd, F.HBlunck, The pyrolysis of esters. *J. Am. Chem Soc.* 60(10) (1938) 2419-2425.
10. J.M. Venon, D. Waddington, Thermolysis of allylicformate. *Journal of Chemical Communication* 11(1969) 623-624.
11. J. H. Warren, *A Guide to molecular Mechanics and Quantum Chemical Calculations*. Irvine USA. P.399.
12. S.W. Benson, *The Foundations of Chemical Kinetics*. Mc-Graw-Hill: New York (1960).
13. C. H. DePuy, R.W. King, Pyrolytics eliminations. *Chem. Rev.*, 60(5) (1960) 431-457.
14. D.A. Mcquarrie, *Molecular Approach, Sausauto*; University Science Books (1997).
15. I.A. Adejoro, O.T. Bamkole, Kinetics and Mechanism of elimination of ethyl acetate in the gas phase: A theoretical study. *Afr. J. Pure Appl. Chem.* 3:7 (2009).
16. K.H. Leavel, E.S. Lewis, Rearrangement of esters in the gas phase, V. Gas-phase thermolysis of allylicformates. Kinetics and isotope effects, *Tetrahedron* 28(1972) 1167–1171.
17. M. Szwarc, J. Watson Taylor, Pyrolyses of benzyl benzoate, acetate, and formate. *J. Chem. Phys.* 21 (1953) 1746–1749.
18. J.R. Mora, D. Perez, A. Maldonado, M. Lorono, G. Chuchani, *Computational and theoretical chemistry* 1019 (2013) 48-58.
19. Spartan Calculation Guide. [www.engin.umich.edu/~cre/web\\_mod/quantum/topic03.htm](http://www.engin.umich.edu/~cre/web_mod/quantum/topic03.htm)
20. Available at: <<https://www.wavefun.com/products/spartan.html>>.